Atlas Journal of Materials Science 2019, pp. 83–89
doi: 10.5147/ajms.v0i0.178

Highly Dense CeO_2 Nano-fibers and MnO_2 Nanoflowers Composite Electrode for Energy Storage Application

Julien C Niyogushima, Makhes K Behera, Samuel A Danquah, Sangram K Pradhan, Messaoud Bahoura

Center for Materials Research, Norfolk State University, 700 Park Avenue, Norfolk, VA, 23504, USA

Received: August 23, 2018 / Accepted: December 9, 2018

Abstract

A high demand of energy storage devices has boosted research for fabricating ultra-efficient supercapacitors with better energy density and cycling stability. Most of metal oxide-based supercapacitors have limited performance because metal oxides are poor electrical conductors, which hinder the optimal output of the device. In this work, we adopted a novel approach to improve the conductivity of the electrodes and charge storing capability of the device by making a hybrid composite structure. Both CeO_2 nanofibers and MnO_2 nano-flower-like structure are developed using low temperature based hydrothermal synthesis route. The structure and morphology of MnO_2 nano-flower-like and CeO_2 nanofibers were characterized by field emission scanning electron microscopy (FESEM). FESEM confirmed highly dense CeO_2 nanofibers that were ultra-thin in diameter and reproducible nanoflowers are formed during MnO_2 synthesis. This composite metal oxide nanostructured electrode made out of CeO_2 and different weight percentage of MnO_2 is a promising material that can operate at higher voltage due to its superior oxidation performance and shows larger specific capacitance value that enables it to hold more charge during operation. This approach boosts the charge storage capability of the composite electrode materials electrochemically as well as by the pseudocapacitive effect obtained from MnO_2 nano-flower-like and CeO_2 nanofibers. Electrochemical measurement of CeO_2 nanofibers and MnO2 nano-flowers-hybrid composite shows improved specific capacitance value with very large cycling stability.

Introduction

Energy has been predicted to be one of the biggest problems that the human race is expected to face within the next 50 years. With the advancement in technologies and industries, there is a very large depletion in the fossil fuel reserves which leaves a void in the sustainable and consistent source of energy. Therefore, it makes it imperative to improve on the existing renewable sources of energy as well as in the energy storage devices (Maheswari and Muralidharan, 2015). Scientists, all across the world, have put in a lot of efforts in finding new materials to improve energy storage devices such as batteries, capacitors and super-capacitors (Shovo et al., 2015).

Super-capacitors have unique properties of fast charging times without being overcharged, a high specific power density and virtually endless cycle life. Moreover, the low resistances in the super-capacitors allow high load currents as well as an excellent low temperature charge-discharge performance. All these properties make super-capacitor to be an ideal candidate for applications in computer systems, medical systems, regenerative braking in automobiles, power supplies, inverters, cameras, welders, uninterruptible power Supply (UPS) systems, audio systems and emergency lighting. However, despite all these advantages, super-capacitors still have limitations in terms of their specific energy, operational voltage window, self-discharge and cycling stability.

Super-capacitors can be classified into two different categories: electrical double layer capacitors (EDLC) and pseudo-capacitors. In electrical double layer capacitors, the charge storing capability comes from the electrostatic charge accumulation at the electrode-electrolyte interface which is a non-faradic

* Corresponding author: j.c.niyogushima@spartans.nsu.edu

process; while the pseudo-capacitors are able to store energy through a fast and reversible faradic reaction, which originate from transition metal oxides or conducting polymers present in the electrode materials (Shovo et al., 2015).

Common metal oxides that have been researched as possible candidates to be used as electrodes in super-capacitors include: RuO_2, MnO_2, NiO, Co_3O_4, SnO_2, ZnO, TiO_2, V_2O_5, CuO, Fe_2O_3, WO_3, etc. (Jadhav et al., 2015). CeO_2 nano-structures have shown a superior oxidation performance and therefore a high specific capacitance (Maheswari and Muralidharan, 2015; Rajib et al., 2015). Although CeO_2 has good redox characteristics, it suffers from poor conductivity and structure stability. Its lattice always expanded when Ce^{4+} was reduced to Ce^{3+}. Consequently, it is not to be used alone for electrode material. To meet the requirement of high-performance super-capacitors, good capacitance performance, rate capability, energy density and cycle stability simultaneously, it is essential to combine CeO_2 with carbon materials or MnO_2 (Maheswari and Muralidharan, 2015; Rajib et al., 2015; Gao et al., 2012). Carbon materials can largely compensate for CeO_2 deficiencies in view of their fine conductivity, developed porosity and large specific surface area (Shuvo et al., 2013). On the other hand, MnO_2 is a highly attractive positive electrode material, benefiting from its low cost, abundance, and remarkable electrochemical performance in aqueous electrolytes. In this study, CeO_2 nano-fibers and MnO_2 nano-structures were grown using a low temperature hydrothermal synthesis route. The electrode for the super-capacitor was fabricated using a hybrid composite of the nano-fibers, conductive porous carbon and long chain polymers. The hybrid composite helps in improving the conductivity of the electrodes as opposed to transition metal oxide and thereby improves the specific capacitance of the super-capacitor.

Materials and Methods

Synthesis of Cerium Oxide Nano-Fibers

Cerium oxide nano-fibers (CeO_2 nano-fibers) were prepared using a one-step hydrothermal method. 6.4 g of sodium hydroxide (NaOH, Sigma-Aldrich, 97%) was dissolved in 16 mL of deionized (DI) water. When solution was clear, 0.5 g of cerium (III) sulfate hydrate Ce2 (SO4)3 (Alfa-Aesar, 99.999%) and 16 mL ethylene glycol (TCI America, >99.0%) were added to the solution under continuous stirring for 2 mins. The solution was then transferred into a Teflon-lined stainless steel autoclave (100 mL). The autoclave was sealed and maintained at 140°C for 12 h. After the reaction was completed, the autoclave was allowed to cool to room temperature naturally. The solid grey precipitate was filtered, washed three times with distilled water and ethanol to removes impurities. Then the precipitate was dried at 60 oC for 12 h to obtain a yellow powder. At last, the product was annealed at 600 oC in air for 1 h. The morphology of the nano-fibers was confirmed using a field emission scanning electron microscope (FESEM) (Chunwen et al., 2004).

Synthesis MnO_2 Nano-Structures

MnO_2 nano-structures were prepared using a facile hydrothermal route. In typical 1.71 g of $MnSO_4$ (Alfa-Aesar, 99.999%) and 2.72 g of KMnO4 (Home Science Tools, 99.99%) were dissolved in distilled water (35 mL) in room temperature and followed by adding 2mL of H_2SO_4 (Fischer Scientific). Stirring the solution for 3 mins in room temperature, the solution was then transferred into a Teflon-lined stainless steel autoclave (100 mL). The autoclave was sealed and maintained at 140°C for 6 h. After the reaction was completed, the autoclave was allowed to cool to room temperature naturally. The solid black precipitate was filtered, washed three times with distilled water and ethanol to removes impurities. Finally the black precipitate was dried in a furnace at 80°C (Bugayeva et al., 2007).

Electrode Fabrication

To fabricate the working CeO_2 electrode, polyvinylidene fluoride (PVDF) (Alfa-Aesar) was used as binding material. Slurry consisting of CeO_2 nano-fibers, PVDF and conductive carbon (Alfa-Aesar, 99%) in a weight ratio of 9:1:1 dissolved in N-Methyl-2-Prorrolidone (NMP) (Alfa-Aesar, 99%) was formed. The slurry was coated on a stainless-steel disk using Doctor Blade's technique and dried at 125°C for 12 h. Similarly, electrodes with CeO_2/MnO_2 composite was prepared by preparing a slurry with CeO_2 nano-fibers and MnO_2 nano-flowers mixed in a ratio of 1:2 (Lin and Chowdhury, 2010; Terribile et al., 1998).

Super-Capacitor Assembly

The super-capacitors were assembled in a coin cell (CR2032) using the electrodes. A 6 M solution of potassium hydroxide (KOH) (Sigma-Aldrich, 99.99%) was used as an electrolyte and commercially available paper towels cut into the size of the coin cell as a separator (Azam et al.; 2013).

Surface Morphology

FESEM by Hitachi SU8010 was used to investigate the surface morphology of all the electrodes prior to assembly into the coin cells to verify the grown nano-structures.

Electrochemical characterization

The fabricated coin cell was characterized for its electrochemical properties using a CH Instruments electrochemical workstation to determine the cyclic voltammetry (CV) and charge-discharge performance.

Results and Discussion

FESEM was used to determine the size and the morphology of the fabricated CeO_2 nano-fibers and electrodes, as shown in Figure 1. As seen from these images, CeO_2 nano-fibers were interconnected between the porous carbons. It was also found

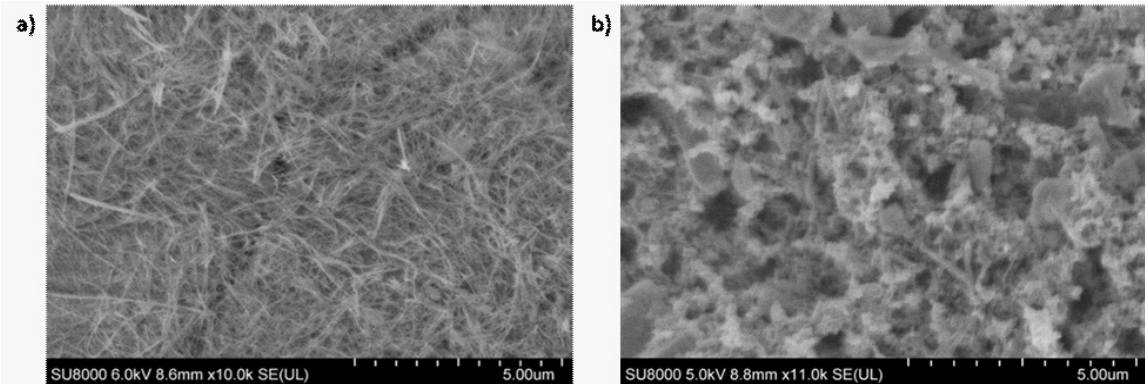

Figure 1. SEM images of (a) hydrothermally grown CeO_2 nano-fibers before addition of porous carbon. (b) Fabricated electrode using CeO_2 nano-fibers with porous carbon.

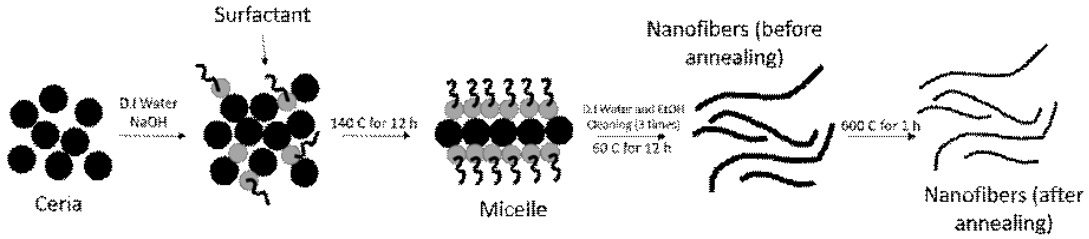

Scheme 1. Details of the reaction mechanism pathways for the formation of CeO2 nano-fibers (Chen et al., 2011).

that the nano-fibers have a diameter less than 30 nm.

Scheme 1 shows the possible reaction scheme with ceria nano-fibers $Ce_2(SO_4)_4$ used as the precursor. Ethyl glycol is absorbed on the surface of CeO_2 nanoparticles (equation (1)). The surfactant plays an important role in the preparation of ceria nano-structure (lin et al.; 2010). Sodium hydroxide and deionized water (D.I.) water were added into precursor (equation (3, 3a, 3b)). Nucleation and growth occurred under hydrothermal conditions at 140°C for 12 h. The solid grey precipitate was washed three times with distilled water and ethanol to remove any impurities. The gray powder was dried at 60°C for 12 h (equation (4)). The product was annealed at 600°C in air for 1 h to remove any organic impurities and to grow CeO_2 nano-fibers (equation (5)). The size and shape of nano-fibers are influenced through the reaction time, reaction temperature and ratio in the initial solution. According to Kuen-Song Lin et al., 2010, the first complete reaction scheme for 1-D ceria preparation in 1998 reported by Terribile et a., 1998.

$$CeOH \rightarrow CeO^- + H^+ \leftrightarrow CeO^- EG^+ \quad (1)$$

According to Terribile et al. (1998), the soluble isolated Ce^{3+}, under basic conditions, oxidizes to a hydrated Ce^{4+} formulated as $Ce(H_2O)_x(OH)_y^{(4-y)+}$, (equation (2))

$$2Ce^{3+} + \frac{1}{2}O_2 \overset{H_2O}{\longleftrightarrow} 2Ce(H_2O)_x(OH)_y^{(4-y)+} \quad (2)$$

Which then readily combines with the surfactant in accordance with reaction, (equation (3a and 3b)),

$$nCe(H_2O)_x(OH)_y^{(4-y)+} \leftrightarrow (-CeHOHOCeHOH)_n.mH_2O + H_2O \quad (3a)$$

This step can also be viewed as the two individual steps for the formation of polymeric hydrous oxide, which then reacts with the soft template as cationic surfactants (ethylene glycol) (equations (3a) and (3b)) at a pH value well above that of the isoelectric point of ceria.

$$(-CeHOHOCeHO\ H)_n.mH_2O + surf \leftrightarrow nCeO_x(O-surf)_y.mH_2O \quad (3b)$$

Under these conditions, surfactant and the deprotonated hydroxyl group form an inorganic/organic composite, which upon drying and calcination (equations (4) and (5)) originates pure mesoporous cerium oxide with high surface area,

$$nCeO_x(O-surf)_y.mH_2O \xrightarrow{drying} nCeO_x(O-surf)_y + mH_2O \quad (4)$$

$$CeO_x(O-surf)_y \xrightarrow{calcination} CeO_2 + org + CO_2 \quad (5)$$

According to reaction (3), Terribile et al. observed that the surfactant is able to promote oxidation of Ce^{3+} to Ce^{4+} and form of hydrous oxide in solution, before drying. The presence of more surface Ce^{4+} atoms is a consequence of the smaller particles formed with the surfactants with a higher number of exposed Ce^{4+} atom (Terribile et al., 1998; Li et al., 2010).

The SEM of MnO_2 nano-structures are displayed in Figure 2. As shown in Figure 2, the morphology of MnO_2 were nano-flowers-like shape with approximately 3 µm, which contains nanorods with uniform length approximately to 2 µm, Figure 2 (a). Figure 2 (b) shows hybrid porous carbon of CeO_2 nano-fibers with between MnO_2 nano-structures.

The scheme 2 illustrates the possible formation process of

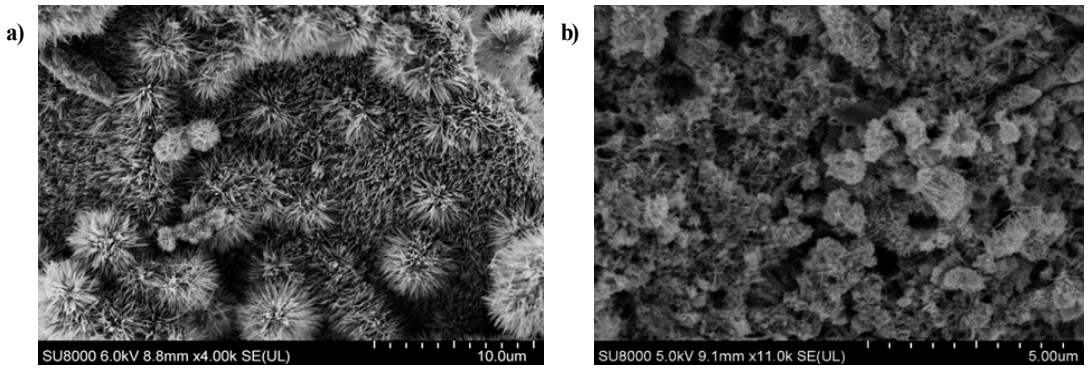

Figure 2. SEM images of hydrothermally grown (a) MnO_2 nano-structures and (b) CeO_2 nano-fibers and MnO2 nano-structures with porous carbon.

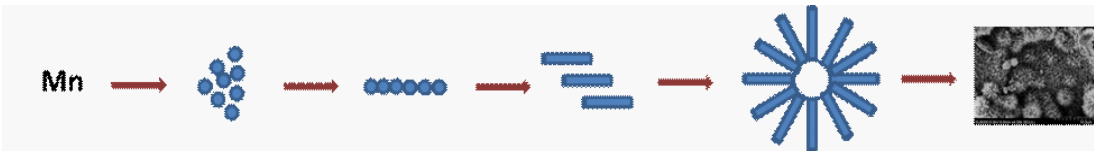

Scheme 2. (b) Reaction mechanism pathways for the formation of MnO2 nano-structures.

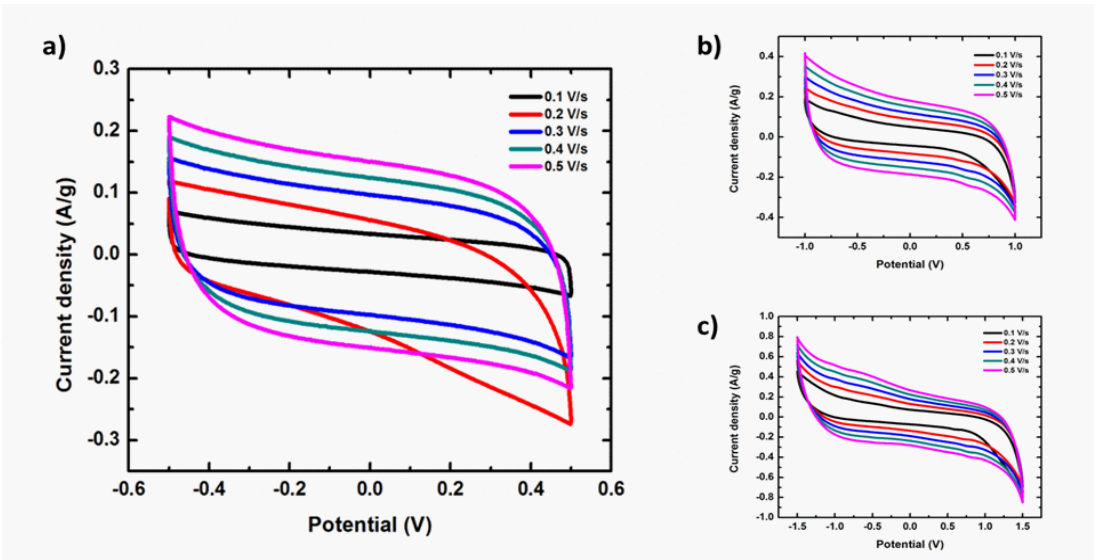

Figure 3 (a-c). Cyclic voltammetry of CeO2 nano-fibers with porous carbon at 1 V, 2 V and 3 V with scan rates of 1 V/s - 5 V/s in an electrolyte of 6M KOH in DI water.

the MnO_2 nano-structures (Feng et al., 2014). During the preparation of the MnO_2 nano-structures, $KMnO_4$ plays the role in oxidating Mn^{2+} ion to MnO_2. Firstly, the tiny crystalline nuclei of MnO_2 are generated from Mn^{2+} by the oxidation in the supersaturated solution and grow into nanoparticles. The nucleation process could be represented as:

$$3MnSO_4 + 2KMnO_4 + 8H_2SO4 + H_2O \xrightarrow{calcination} 5Mn(SO_4)_2 + K_2SO_4 + 9H_2O \quad (6)$$

Therefore, sulfuric acid is added to decrease the reaction rate, and the morphology can be modulated. The tiny nanoparticles spontaneously aggregate into long nanowires. With minimizing interfacial energies, the nanowires wrap with each other incompactly to form a flowers-shaped MnO_2 nano-structures.

CV and galvanostatic charge/discharge were used to understand the electrochemical behavior for the CeO_2 nano-fibers with porous carbon. 6 M KOH in DI water was used as the electrolyte solution. Coin cell was assembled using CeO_2 nano-fibers with porous carbon electrode. Figure 3 (a-c) show CV at different scan rates of 1 V/s, 2 V/s, 3 V/s, 4 V/s and 5 V/s with voltage windows between 1 to 3V. The area under each CV curve suggests that super-capacitor have a good electrochemical stability (Mendoza et al., 2012; Chena et al., 2011).
Specific capacitance, Cs (Fg-1) for super-capacitor was calculate by the following equation:

$$C_s = \frac{4I}{m}\frac{\Delta t}{\Delta V} \quad (7)$$

Where I is the discharge current (A), m is the mass of active material (g), Δt is the discharge time (secs), and ΔV is the

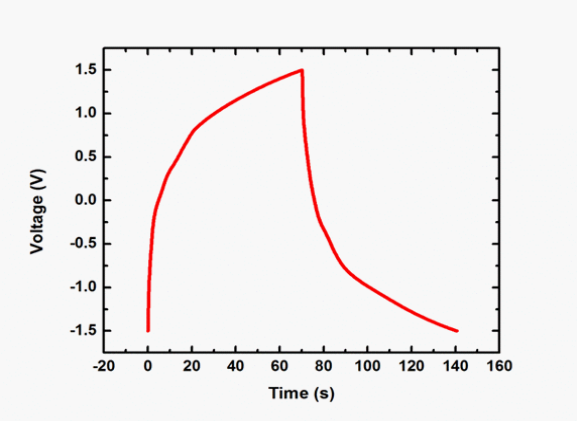

Figure 4. Galvanostatic charge discharge for CeO_2 at a potential window of 3 V with a discharge current of 0.25 A/g.

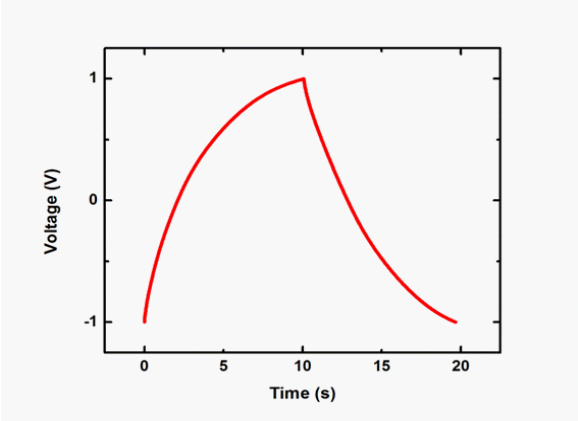

Figure 6. Galvanostatic charge discharge of CeO_2 nano-fibers and MnO_2 nano-structures (1:1 ratio) with porous carbon at a potential window of 2 V with a discharge current of 0.25 A/g.

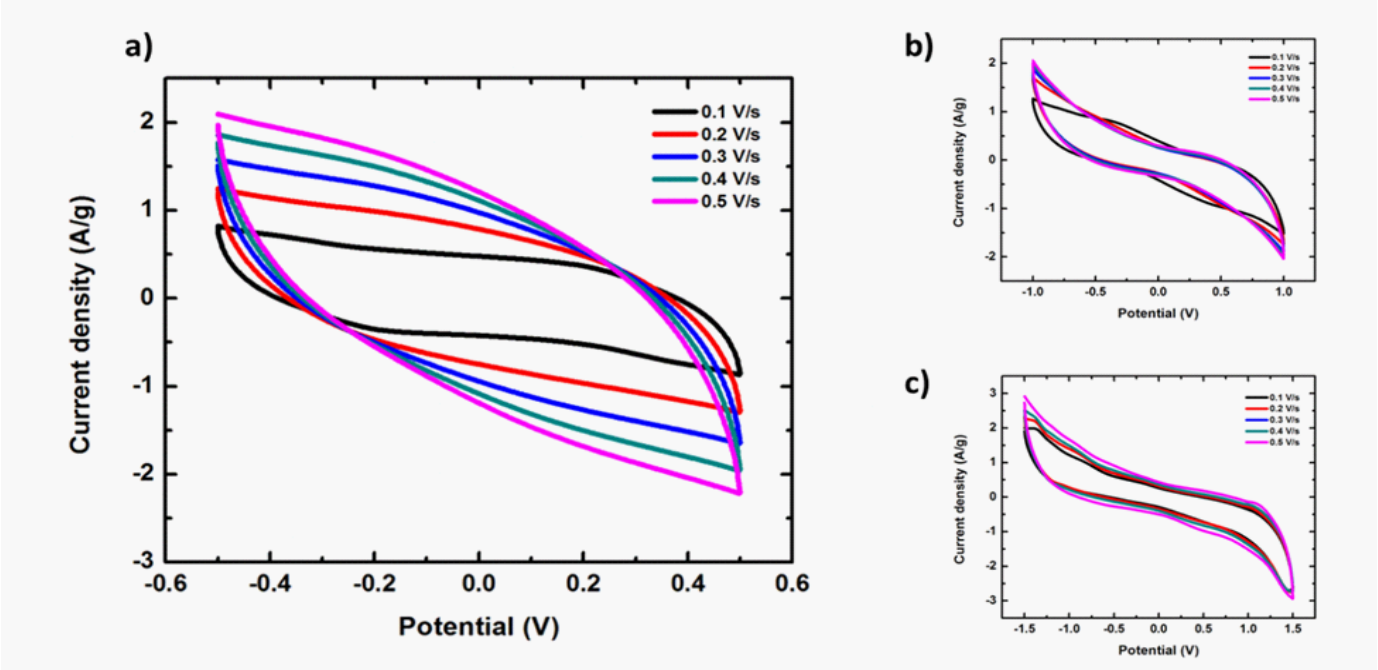

Figure 5. (a-c) Cyclic voltammetry of CeO2 nano-fibers and MnO2 nanoflowers (1:2 ratio) with porous carbon at scan rates of 1 V/s - 5 V/s in an electrolyte of 6 M KOH in D.I. water.

discharge voltage (V).

Figure 4. Shows the galvanostatic charge discharge curves for CeO_2 nano-fibers with porous carbon with potential voltage window of 1 V, 2 V and 3 V. The charge and discharge showed a symmetrical behavior which indicates the good electrochemical capacitive property and high reversibility (Shovo et al 2013; Chena et al., 2011; Gao et al., 2012).

CeO_2 nano-fibers and MnO_2 nano-structures were used to understand the role of CeO_2 nano-fibers in electrochemical performance. Fig 5 (a-c), 6, 7 (a-c) and 8 show the CV and galvanostatic charge/discharge of CeO_2 nano-fibers and MnO_2 nano-structures with porous carbon with 3:9:1 ratio. A 6 M KOH in D.I. water was used as the electrolyte solution for assembling electrode testing set up as coin cells. Figure 5 (a-c) shows cyclic voltammetry at different scan rates of 1 V/s, 2 V/s, 3 V/s, 4 V/s and 5 V/s with a voltage window between 1 to 3V.

The specific capacitance of CeO_2 nano-fibers and MnO_2 nano-structures (1:1 ratio) with porous carbon was found to be 4.81 F/g at 2 V, compared to the specific capacitance of CeO_2 nano-fibers with porous carbon, which was 23.7 F/g at 3 V.

The specific capacitance of CeO_2 nano-fibers and MnO_2 nano-structures (1:2) with porous carbon were 162.6 F/g at 1.48 V compared to the specific capacitance of CeO_2 nano-fibers with porous carbon which were 23.7 F/g at 3 V. Figure 8 shows the galvanostatic charge discharge of CeO_2 nano-fibers and MnO_2 nano-structures (1:2 ratio) with porous carbon.

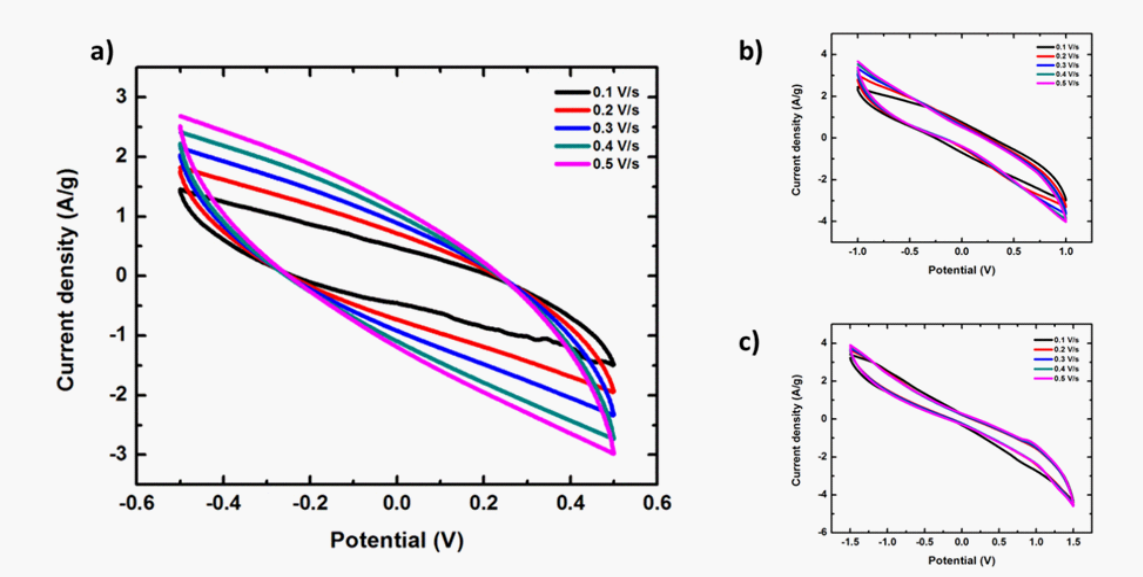

Figure 7. Galvanostatic charge discharge of CeO2 nano-fibers and MnO2 nano-structures (1:1 ratio) with porous carbon at a potential window of 2 V with a discharge current of 0.25 A/g.

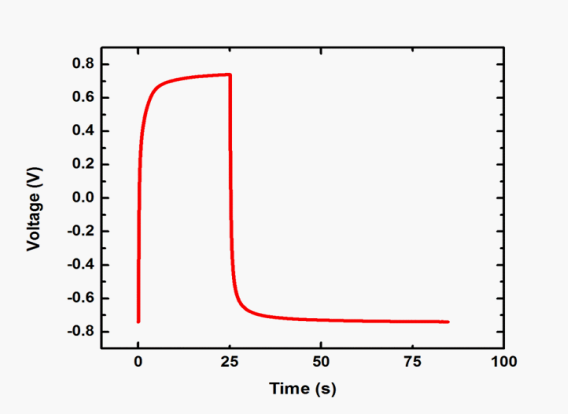

Figure 8. Galvanostatic charge discharge of CeO_2 nano-fibers and MnO_2 nano-structures (1:2 ratio) with porous carbon at a potential window of 1.48 V with a discharge current of 1 A/g.

Conclusion

We report on a novel approach to improve the conductivity of the electrodes and charge storing capability of the device by making a hybrid composite structure with conducting porous carbon and long chain polymers through a simple, efficient and low temperature based hydrothermal synthesis route. The formation of thin (less than 30 nm in diameter) nano-fibers with long length enabled us to improve on the charge storage efficiency of the device as confirmed by the FESEM images. The simplicity and the efficiency of the process still leaves room for improvement to the nano-structure of the hydrothermally grown CeO_2 that can, possibly, lead to an improvement to the specific capacitance and operating voltage window of the super-capacitors.

Acknowledgments

This work is supported by the NSF-CREST Grant number HRD 1547771 and NSF-CREST Grant number HRD 1036494.

References

Azam, Mohd Asyadi, Akihiko Fujiwara, and Tatsuya Shimoda (2013) Significant capacitance performance of vertically aligned single-walled carbon nanotube supercapacitor by varying potassium hydroxide concentration. Int. J. Electrochem. Sci 8 (3): 3902-3911.

Bugayeva, N., and J. Robinson (2007) Synthesis of hydrated CeO_2 nanowires and nanoneedles." Materials science and technology 23 (2): 237-241.

Chen, Ying-Chu, Yu-Kuei Hsu, Yan-Gu Lin, Yu-Kai Lin, Ying-Ying Horng, Li-Chyong Chen, and Kuei-Hsien Chen (2011) Highly flexible supercapacitors with manganese oxide nanosheet/carbon cloth

electrode." Electrochimica Acta 56 (20): 7124-7130.

Feng, Lili, Zhewen Xuan, Hongbo Zhao, Yang Bai, Junming Guo, Chang-wei Su, and Xiaokai Chen (2014) MnO_2 prepared by hydrothermal method and electrochemical performance as anode for lithium-ion battery." Nanoscale Research Letters 9 (1): 290.

Gao, Hongcai, Fei Xiao, Chi Bun Ching, and Hongwei Duan (2012) High-performance asymmetric supercapacitor based on graphene hydrogel and nanostructured MnO_2. ACS applied materials & interfaces 4 (5): 2801-2810.

Jadhav, Vijaykumar V., Manohar K. Zate, Shude Liu, Mu Naushad, Rajaram S. Mane, K. N. Hui, and Sung-Hwan Han (2016) Mixed-phase bismuth ferrite nanoflake electrodes for supercapacitor application. Applied Nanoscience 6 (4): 511-519.

Lin, Kuen-Song, and Sujan Chowdhury (2010) Synthesis, characterization, and application of 1-D cerium oxide na1nomaterials: a review. International Journal of Molecular Sciences 11 (9): 3226-3251.

Maheswari, Nallappan, and Gopalan Muralidharan (2015) Supercapacitor behavior of cerium oxide nanoparticles in neutral aqueous electrolytes. Energy & Fuels 29 (12): 8246-8253.

Mendoza, Miguel, Md Ashiqur Rahaman Khan, Mohammad Arif Ishtiaque Shuvo, Alberto Guerrero, and Yirong Lin (2012) Development of lead-free nanowire composites for energy storage applications. SRN Nanomaterials 2012.

Pan, Chengsi, Dengsong Zhang, and Liyi Shi (2008) CTAB assisted hydrothermal synthesis, controlled conversion and CO oxidation properties of CeO_2 nanoplates, nanotubes, and nanorods. Journal of solid state chemistry 181 (6): 1298-1306.

Rajib, Md, Mohammad Arif Ishtiaque Shuvo, Hasanul Karim, Diego Delfin, Samia Afrin, and Yirong Lin (2015) Temperature influence on dielectric energy storage of nanocomposites. Ceramics International 41 (1): 1807-1813.

Shuvo, Mohammad Arif Ishtiaque, Hasanul Karim, Md Tariqul Islam, Gerardo Rodriguez, Manjula I. Nandasiri, Ashleigh M. Schwarz, Arun Devaraj, Juan C. Noveron, Murugesan Vijayakumar, and Yirong Lin (2015) High-performance porous carbon/CeO_2 nanoparticles hybrid super-capacitors for energy storage. In Smart Materials and Nondestructive Evaluation for Energy Systems 9439, p. 94390H. International Society for Optics and Photonics.

Shuvo, Mohammad Arif Ishtiaque, Tzu-Liang Tseng, Md Ashiqur Rahaman Khan, Hasanul Karim, Philip Morton, Diego Delfin, and Yirong Lin (2013) Nanowire modified carbon fibers for enhanced electrical energy storage. Journal of Applied Physics 114 (10): 104306.

Shuvo, Mohammad Arif Ishtiaque, Tzu-Liang Tseng, Md Ashiqur Rahaman Khan, Hasanul Karim, Philip Morton, Diego Delfin, and Yirong Lin. "Nanowire modified carbon fibers for enhanced electrical energy storage." Journal of Applied Physics 114, no. 10 (2013): 104306.

Sun, Chunwen, Hong Li, ZhaoXiang Wang, Liquan Chen, and Xuejie Huang (2004) Synthesis and characterization of polycrystalline CeO_2 nanowires. Chemistry Letters 33 (6): 662-663.

Terribile, Daniela, Alessandro Trovarelli, Jordi Llorca, Carla de Leitenburg, and Giuliano Dolcetti (1998) The synthesis and characterization of mesoporous high-surface area ceria prepared using a hybrid organic/inorganic route." Journal of Catalysis 178 (1): 299-308.

Wang, Hsien-Cheng, and Chung-Hsin Lu (2002) Synthesis of cerium hydroxycarbonate powders via a hydrothermal technique. Materials Research Bulletin 37 (4): 783-792.

Yada, Mitsunori, Seiji Sakai, Toshio Torikai, Takanori Watari, Sachiko Furuta, and Hiroaki Katsuki (2004) Cerium compound nanowires and nanorings templated by mixed organic molecules. Advanced Materials 16 (14): 1222-1226.

Yan, Lai, Xianran Xing, Ranbo Yu, Jinxia Deng, Jun Chen, and Guirong Liu. "Facile alcohothermal synthesis of large-scale ceria nanowires with organic surfactant assistance. Physica B: Condensed Matter 390 (1-2): 59-64.

Yang, Ru, and Liang Guo (2004) Synthesis of the Nanotublar Cubic Fluorite CeO_2. Chinese Journal of Inorganic Chemistry 20 (2): 152-158.